A quantitative measure of functional redundancy in microbial ecosystems

Taylor M. Royalty (1) and Andrew D. Steen (2,1)*

University of Tennessee Departments of (1) Earth and Planetary Sciences and (2) Microbiology

Running title:

Measuring the functional redundancy of microbiomes

*Corresponding: asteen1@utk.edu

Abstract

Although functional redundancy has received increased attention in the microbial ecology literature, no quantitative functional redundancy measurement is currently available which compares multiple communities and integrates of ‘omics data rather than phenotypic traits. Here, we propose an approach for quantifying functional redundancy that use ‘omics data. This approach, termed trait contribution evenness (TCE), is based on traditional measures of community diversity. We measure functional redundancy of a trait within a community as the evenness in relative contribution of that trait among taxa within the community. This definition has several appealing properties including: TCE is an extension of established diversity theory, functional redundancy measurements from communities with different richness and relative trait contribution by taxa are easily comparable, and any quantifiable trait data (genes copies, protein abundance, transcript copies, respiration rates, etc.) is suitable for analysis. Resilience of a trait to taxa extinctions is often viewed as an ecological consequence of traits with high functional redundancy. We demonstrate that TCE functional redundancy is closely and monotonically related to the resilience of a trait to extinctions of trait-bearing taxa. Finally, to illustrate the applicability of TCE, we analyzed the functional redundancy of eight nitrogen-transforming pathways using 2,631 metagenome-assembled genomes from 47 TARA Oceans sites. We found that the NH_4^+ assimilation pathway was the most functionally redundant (0.6 to 0.7) while nitrification had the lowest functional redundancy (0 to 0.1). Here, TCE functional redundancy addresses shortfalls of other functional redundancy measurements by providing a generalizable, quantitative, and comparable functional redundancy measurement.

Importance

The broad application of ‘omics technologies in microbiological studies highlights the necessity of integrating traditional ecological theory with omics data when quantifying community functional redundancy. Such an approach should allow for comparisons in functional redundancy between different samples, sites, and studies. Here, we propose measuring functional redundancy based on an expansion of already existing diversity theory. This approach measures how evenly different members in a community contribute to the overall level of a trait within a community. The utility in the approach proposed here will allow for broad evaluation of traits.

Introduction

In recent years, the emergence of ‘omics technologies has greatly improved microbial ecologists’ ability to evaluate the relationships between phylogeny, trait distributions and environmental gradients (1–4). Such studies have frequently found that ecosystem functions are frequently performed simultaneously by many taxa (5). This is referred to as functional redundancy (6).

The level of functional redundancy in a microbiome has been shown to affect ecosystem function in diverse environments. For instance, high functional redundancy in freshwater sediments resulted in stabilized porewater redox conditions (7). In surface seawater, a metagenomic analysis of glycosyl hydrolase genes demonstrated a complex successional pattern in heterotrophs which correlated with coastal phytoplankton bloom life cycles and influenced ecosystem organic carbon processing (8). In the case of human gut microbiomes, it has been hypothesized that functional redundancy stabilizes community diversity leading to better health (9).

A quantifiable and comparable measure for functional redundancy is a prerequisite in addressing ecological questions pertaining to functional redundancy. Concepts related to functional diversity and redundancy have been actively discussed in the macroecology literature for over 40 years (6, 10, 11). Nonetheless, there remains no universal method to quantify functional redundancy (11–14). Many of the most popular methods rely on measuring dissimilarity in traits between community members. Dissimilarities are then adjusted to consider the community member relative abundances. Most notably, the normalization of Rao’s quadratic diversity by Simpson’s index has been used as a quantitative measure of functional redundancy (11). In this approach, functional redundancy is quantified as the average similarity in relative

trait contribution by different taxa. However, this approach does not appear sensitive changes in concavity and convexity of community trait distributions, as demonstrated here.

In principle, methods to quantify functional diversity in macro-ecosystems should be equally applicable to microbial ecosystems. In practice, the measurement of microbial community composition and trait distribution possess unique challenges. In macro-ecosystems, tens or hundreds of species might be considered, and traits are often determined from direct field observations. In microbial ecosystems, millions of unique taxa may be present, and the appropriate level of taxonomic organization (i.e., amplicon sequence variant, operational taxonomic unit defined by a semi-arbitrary cutoff of 16S rRNA gene similarity) depends on experimental design. Traits, such as net respiration or nutrient uptake rates, are sometimes directly measurable but linking rates of specific biogeochemical transformations to specific taxa is a challenging exercise. Most microbial cells on Earth belong to genera which lack cultured representatives, so the traits of most members of microbiomes are frequently unknown (15). Consequently, the microbiological community relies on ‘omics technology (genes, transcripts, or proteins) to characterize community function. This reality necessitates a functional redundancy measurement suitable for both ‘omics and phenotypic data.

Microbial ecologists have typically addressed these problems using two broad approaches. One common method is to compare changes in ecosystem function to changes in community composition. Stability in ecosystem function with increasing microbial diversity is often considered an empirical indication of functional redundancy (7, 16, 17). A complimentary approach is to use ‘omics data as indicators of traits (18, 19). The presence of similar traits in distinct taxa is taken as evidence of functional redundancy. This approach may stretch the definition of trait, as ‘omics data do not guarantee a phenotypic response. Nonetheless, this

second approach circumnavigates the lack of taxa-specific physiological data for most environmental microbiomes. Overall, these approaches are conceptually straightforward but are largely qualitative and yield results that are challenging to compare among studies.

Here, we use diversity theory (20) to establish a quantitative approach to measure functional redundancy of microbiomes using ‘omics data, which includes metagenomes, metatranscriptomes, and metaproteomes. We argue that functional redundancy is best understood as the evenness of the contribution of taxa to a community-wide trait. Communities are functionally redundant if taxa contribute equally to an ecosystem function (6, 16). We measured this by first defining two measures of abundance: taxa abundance distributions and trait abundance distributions, or levels. Taxa abundance distributions correspond to conventional species abundance distributions (21). Trait abundance distributions correspond to relative trait levels for individual taxa, i.e., the total amount of a trait in taxon. By taking the product of these two abundance distributions, we measured the relative contribution by taxa to the overall trait within a community, or the trait contribution distribution.

Traditional approaches for measuring diversity and evenness are applicable to trait contribution distributions, as the trait contribution distribution fulfills mathematical properties defining a community (20). We find trait contribution evenness (TCE) appealing because it is easily generalizable. Theoretically, any type of trait data can be used with this approach (e.g., gene copies, enzyme kinetics, nutrient uptake, etc.) if the trait can be assigned to taxa and the relative abundance of those respective taxa are known. We demonstrated the efficacy of TCE by correlating functional redundancy against a conceptual idea commonly associated with functional redundancy, the risk of losing ecosystem function due to taxa extinction. Lastly, we analyzed functional redundancy for eight nitrogen-transforming pathways found in metagenomic

data (22) in *TARA* Oceans draft metagenome-assembled genomes (MAGs) (23). We hope that the formulation of functional redundancy presented here fills a void in the microbial ecology literature by providing a generalized tool for generating higher quality measurements of an important parameter in microbial communities.

Results and Discussion

Representing microbial communities as taxa abundance, trait abundance, and trait contribution distributions

We represent microbial community traits using two distributions: the distribution of taxon abundance within the community, and the distribution of trait quantity among each taxon (Fig 1A). We define 'trait' liberally to include genes, transcripts, or proteins ("potential traits"). This definition has been adopted in many studies when inferring microbially-mediated biogeochemistry and microbial ecology (e.g., 23–26). Furthermore, traits encompass processes catalyzed by microbes such as nutrient uptake or respiration ("realized traits"). The choice of traits to analyze is always central in experimental design. However, for the purposes of the method described here, traits may represent anything that can be quantifiably apportioned among taxa, including binary presence/absence apportionments.

Since trait levels are measured as non-negative, real numbers, both taxa relative abundances (equation 1) and trait abundances (equation 2) can be represented as relative abundance distributions (Fig 1B). We determined the relative contribution of individual taxa to the total, community-wide trait level from the product of taxon relative abundances and their respective trait abundance distributions (equation 3). We refer to the distribution of the relative contribution of each taxon to total, community-wide trait level as the trait contribution

distribution (equation 4). Thus, an abundant taxon that expresses a small amount of trait per cell might contribute equally to the total trait level within a community as a rarer taxon that expresses a large amount of trait per cell (Fig 1B). In cases of presence/absence trait data, the trait contribution distribution reflects the relative abundance of trait-containing taxa.

Defining and Quantifying Functional Redundancy

We define functional redundancy as how evenly taxa in a community contribute to the total quantity of trait exhibited by the community. A community in which each taxon contributes an equal quantity of trait would be maximally functionally redundant with respect to the trait. For example, a community of heterotrophs in which each taxon consumes oxygen at an equal rate would be maximally redundant with respect to oxygen consumption. Conversely, if that community contained a single taxon capable of fixing nitrogen, that community would be minimally redundant with respect to nitrogen fixation.

The trait contribution distribution (equation 4) provides an invaluable tool for visualizing trait functional redundancy within a community, as these distributions allow for pairwise comparisons in relative trait contribution by different taxa. Comparative analyses of trait contribution distribution from multiple communities may be difficult due to differences in structure and richness. Similar challenges exist when comparing diversity between taxa abundance distributions (20). Consequently, diversity indices have become elegant solutions for comparing community diversity among different communities, as variations in taxa abundance are collapsed into a singular value. The applicability of diversity indices extends beyond taxa abundance distributions and includes any categorical abundance vector (20). The generalizability of diversity indices, along with the fact that diversity indices are used for measuring community evenness (28), prompted us to explore using diversity metrics to quantify functional redundancy.

We quantified the diversity of trait contribution distributions (equation 4) using traditional diversity indices (equation 5). Numerous diversity indices have been proposed in the literature. Three common measures of diversity, taxa richness, Shannon's diversity index, and Simpson's diversity index, are manifestations of the parametric diversity index, in which the α parameter determines the relative weight placed on rare versus common taxa. Equation 5 with α=0 becomes the sum of taxa present in a sample, or taxon richness. When α=1 or 2, equation 5 becomes the equation for Shannon's and Simpson's diversity indices respectively. We adopted the parametric diversity index for this flexibility in weighting the importance of taxa. An evaluation of their viability demonstrated thermophiles did not contribute to biogeochemical processes (29). Next, we quantified a theoretical maximum diversity for the same trait contribution distributions assuming relative contribution of traits were evenly spread among all taxa (equation 6). Community evenness can be derived by taking the ratio of community diversity to the theoretical maximum diversity (28). As such, we normalized diversity of the trait contribution distribution by the theoretical maximum diversity (equation 7). We refer to this statistical measure (equations 5-7) of the trait contribution distributions as trait contribution evenness (TCE). TCE measured of how evenly taxa contribute to a specific trait within the community, or the functional redundancy of the trait. TCE differs from other proposed methods measuring functional diversity, richness, and redundancy as these methods use distance-based methods (11, 13, 14), rely on empirical changes in realized traits with respect to community diversity (7, 17), or pairwise comparisons in trait levels (18, 25) when analyzing the trait contribution distributions. In order to facilitate the use of TCE functional redundancy measurements, we have provided an R script to calculate TCE functional redundancy at https://github.com/taylorroyalty/functional_redundancy_script.

Influence on Functional Redundancy from Taxa Lacking the Trait

We quantified the diversity of trait contribution distributions (equation 4) using traditional diversity indices (equation 5). Numerous diversity indices have been proposed in the literature. Three common measures of diversity, taxa richness, Shannon's diversity index, and Simpson's diversity index, are manifestations of the parametric diversity index, in which the α parameter determines the relative weight placed on rare versus common taxa. Equation 5 with α=0 becomes the sum of taxa present in a sample, or taxon richness. When α=1 or 2, equation 5 becomes the equation for Shannon's and Simpson's diversity indices respectively. We adopted the parametric diversity index for this flexibility in weighting the importance of taxa. An evaluation of their viability demonstrated thermophiles did not contribute to biogeochemical processes (29). Next, we quantified a theoretical maximum diversity for the same trait contribution distributions assuming relative contribution of traits were evenly spread among all taxa (equation 6). Community evenness can be derived by taking the ratio of community diversity to the theoretical maximum diversity (28). As such, we normalized diversity of the trait contribution distribution by the theoretical maximum diversity (equation 7). We refer to this statistical measure (equations 5-7) of the trait contribution distributions as trait contribution evenness (TCE). TCE measured of how evenly taxa contribute to a specific trait within the community, or the functional redundancy of the trait. TCE differs from other proposed methods measuring functional diversity, richness, and redundancy as these methods use distance-based methods (11, 13, 14), rely on empirical changes in realized traits with respect to community diversity (7, 17), or pairwise comparisons in trait levels (18, 25) when analyzing the trait contribution distributions.

We created a simulation which we increased taxa richness (n) while fixing the richness of taxa containing a trait (ν) and the relative trait contribution by these taxa (τ) (equation 3-4). The parametric diversity index requires selecting a value for the parameter, α, which varies the

sensitivity that the measured functional redundancy has to community taxa contributing less to the overall community trait level. We performed the simulations such that the parameter, α, varied from 0 to 2 for each combination of total taxa richness and trait-containing taxa richness (Fig 2). Functional redundancy was less sensitive to increasing taxa richness for larger α values. When the community structures are fixed (equations 1 and 2, respectively), the functional redundancy values derived from different α values are correlated very closely to one another. To emphasize this point, we plotted select α from contours in Fig 2A across all taxa richness (Fig 2B-C); these plots were nearly linear. Thus, α represents a parameter which simply augments values of functional redundancy and is not a parameter reflecting ecological significance. We recommend that if influences from high beta-diversity in non-trait containing taxa is not desirable in calculating functional redundancy, then α values closer to 2 should be used in equation 5.

When evaluating functional redundancy in real biological systems, it may be desirable to relate functional redundancy to environmental factors such as nutrients or temperature. The sensitivity that functional redundancy relates to these parameters depends on the α parameter (Fig 2). Another consideration (beyond functional form) includes the influence that the α parameter has on the range in precision, or dynamic range, of functional redundancy. Specifically, the maximum and minimum values of functional redundancy are one and zero, respectively. However, an increase in precision when converging towards zero may be useful to prevent a loss in functional redundancy sensitivity to exogeneous factors. We evaluated the dynamic range in functional redundancy for 10,000 randomly generated artificial communities as a function of the α parameter. Functional redundancy spanned up to ~10 orders of magnitude depending on the choice in α parameter as well as the fraction of taxa with the trait (Fig 3). The

functional form for dynamic range varied depending on the fraction of taxa with the trait. Communities where all taxa had the trait behaved had a local maximum while communities with <100% of taxa were asymptotic. Nonetheless, the maximum dynamic range for all considered scenarios occurred at $\alpha<1$. This implies that a greater range of functional redundancy values can be measured, if the diversity index provides low to moderate weighting for taxa with lower trait contribution towards the overall community trait level. A selection of $1\geq\alpha\geq0.5$ appeared adequate if making comparisons between communities with drastically different ratios of trait-containing richness taxa richness (v) and taxa richness (n).

Functional Redundancy and Trait Resilience to Taxa Extinction

One tangible ecological consequence of functional redundancy is increased resilience of biogeochemical functions to taxon extinction. When functions are more broadly distributed across taxa, a function is less likely to disappear due to the extinction of individual taxa. This interpretation is often highlighted in macro-ecological studies (11, 30, 31). Therefore, any measure of functional redundancy should reflect that the probability of a trait being extinguished from a community decreases as the redundancy of that trait within the community increases.

The conceptual relationship between functional redundancy and vulnerability of ecosystem function provides an opportunity to demonstrate the efficacy in TCE. To do this, functional redundancy was calculated for randomly generated communities, which followed lognormal distributions (21, 32) (equation 8). Individual taxa were randomly assigned a trait level. We simulated random taxon extinction events in the artificial communities until >95% of the original community total trait was gone. The choice in threshold served the purpose of dealing with communities where all taxa possessed a trait. In such communities, a 100% extinction rate was necessary to properly remove the trait from the community. In real biological

systems, an ecosystem function may be disrupted well before all taxa contributing to a trait are extinct. For instance, porewater redox conditions become temporally unstable with minor losses in organoheterotroph composition (7). For our calculation of equation 5, we selected α=0.5 because it maximized the observable dynamic range of the functional redundancy parameter (Fig 3). We observed a positive relationship between the resilience of a trait to random taxon extinction events and the calculated functional redundancy (Fig 4A). In addition to TCE, we evaluated the formulation for functional redundancy presented in (11) to draw comparison. As a general observation, this method performed poorly as no clear functional relationship existed between estimates in functional redundancy and trait resilience to extinction (Fig 4B). We suspect the discrepancy in performance between TCE and the method from (11) is explained by TCE's use of diversity to quantify functional redundancy. Specifically, the parametric diversity index (equation 5) is sensitive to the shape of the distributions of species abundance and trait contribution. These properties likely manifest in our extinction simulation, which is a hypergeometric probability distribution problem, weighted proportionally to the trait contribution distribution. In contrast, the formulation in (11) is a measure of mean dissimilarity in trait contribution, and does not account for non-normal abundance distribution shapes.

We ensured the relationship between TCE and trait resilience was not an artifact of α selection. This was done by testing a range of α values against trait resilience to taxa extinction (Fig S1). The relationship between functional redundancy and resilience to extinction remained positive for all evaluated values of α (0.1, 1, and 2). The functional form (e.g., exponential-like versus linear) between functional redundancy and resilience to extinction as well as variance in residuals differed depending on α value selection. Depending on the work, the relationship

between functional redundancy and resilience to extinction may matter, and so flexibility in α selection may prove useful.

Case Study: Redundancy of nitrogen cycle marker genes in marine microbiomes

To demonstrate a use of TCE, we measured functional redundancy in the marine nitrogen cycle using genomic data from the *TARA Oceans* project (4). (23) recently published 2,361 draft metagenome-assembled genomes (MAGs) which represent genomic content from seven oceanographic provinces, three different depths, and four filter size fractions. Relative abundance data used here was reported in (23) and was determined by the proportion of sequence reads mapping to assembled MAGs. For simplicity, we limited our analysis to only MAGs identified in the bacterial size fraction (<3μm), which corresponds to free-living microbes. The nitrogen cycle was simplified to eight pathways (22) and included N_2 fixation, nitrification, NO_3^- reduction, dissimilatory NO_3^- reduction, assimilatory NO_3^-/NO_2^- reduction, NH_4^+ assimilation, N remineralization, and denitrification. A general summary of the marker genes (downloaded from Swiss-Prot; see Methods) used for quantifying nitrogen cycle pathways in MAGs is summarized in Table 1.

Overall, the functional redundancy for individual traits was consistent with our conceptual understanding of primary nitrogen-transforming pathways in the ocean (Fig 5). A clear example was the low functional redundancy in the nitrification pathway. This observation is expected as primary oceanic nitrifying phylum is *Crenarchaeota* (33). Similarly, the N_2 fixation pathway, which is predominantly facilitated by a small group of *Cyanobacteria* (22), exhibits low functional redundancy. Conversely, the uptake of inorganic N via NH_4^+ and NO_3^- /NO_2^- assimilation are broadly expressed traits and should exhibit higher levels of functional redundancy (22). Lastly, the low functional redundancy in dissimilatory NO_3 reduction and NO_3

reduction were not surprising considering these pathways occur in anaerobic and low-oxygen environments, respectively (22).

Some variance existed across oceanographic provinces and depth for intra-pathway functional redundancy (α=0.5). However, inter-pathway variance in functional redundancy was generally larger compared to intra-pathway variance in functional redundancy (Fig 5). This suggests that the marine nitrogen cycle marker genes considered here are consistently distributed within communities for MAGs retrieved in Earth's ocean. This was consistent with the lack of relationship between the metagenome companion metadata (e.g., O_2, inorganic N, PO_4^{3-}, latitude, longitude, etc.) and functional redundancy. This is not particularly surprising as saline water biomes exhibit the lowest alpha-diversity (not to be confused with the α parameter in equation 5) and largely constrained beta-diversity among free-living microbiomes (34). An earlier analysis qualitatively demonstrated similar KEGG ontology in *TARA Oceans* metagenomes, regardless of oceanographic province or depths (4).

In our analysis of *TARA Oceans* metagenomes, traits were loosely defined such that redundancy in function may be observed based on genomic potential. As a point of emphasis, measurable properties (e.g., nitrogen uptake) provide direct measures of ecosystem function which are more easily integrated into predictive numerical models. In an ideal scenario, the latter would be discernible in all ecological studies, for all ecosystem functions. However, the disproportionate number of lineages which lack cultured representatives highlights the continued importance of nucleotide sequencing in microbial ecology (35, 36). Thus, this observation necessitates the development of ecological theory which is inclusive to potential traits as well as realized traits. For instance, technological advances with single-cell nanoSIMS may provide a method for quantifying lineage-specific metabolic rates for *in situ* inoculation studies (37).

Coupling these metabolic rates with abundance data, we believe functional redundancy can be measured for realized traits with TCE.

Methods and Theory

Definition of Functional Redundancy

Here, we present the underlying theory used to quantify functional redundancy. Functional redundancy was defined as how evenly community members contribute to a net trait within the community. Community members represent the aggregation of individuals within phylogenetic clades of a predefined taxonomic level, and thus, are referred to as taxa from henceforth. As this definition of functional redundancy is a measure of the evenness in trait contribution from individual taxa, we propose adapting traditional approaches of measuring diversity and evenness for quantifying functional redundancy. Specifically, we adopt the parametric diversity index due to the degree of generalizability. Consequently, relative trait contribution by taxa to a net trait on a community level has to be expressed as an abundance distribution (20), or the trait contribution distribution.

Here, we define a microbial community, *C*, with *n* taxa, each with a relative abundance of p_i. Thus, the set of taxa in *C* can be described as follows:

$$C = \{p | p_i > 0 \; \forall \; p_i ; \sum_{i=1}^{n} p_i = 1\} \qquad (1$$

where *p* is the set of relative abundances of taxa, such that any given relative abundance for the ith taxon is greater than zero and all taxa relative abundances sum to one. Equation 1 represents a traditional abundance distribution (21).

Taxa in C cumulatively contribute to a net trait, T, which reflects the quantity of a trait on the community level. Units of T are flexible such that T can be expressed in terms of rates (e.g., g C m^{-2} $year^{-1}$ for net primary productivity), quantities (e.g., gene copies), or dimensionless numbers; however, T must be quantitative. Our goal was to express the community, C (equation 1), in terms of the relative contribution by individual taxa towards a total trait, T, at a fixed time and space. This requires knowing the taxa-specific trait level, t_i, and the respective taxa relative abundance, p_i. If the distribution of taxa-specific trait levels, t_i, are known, then relative abundances in equation 1 can be substituted with t_i such that:

$$C_t = \{t | t_i \geq 0 \; \forall \; t_i; \textstyle\sum_{i=1}^{n} t_i = T\} \qquad (2$$

where C_t is the distribution of t across all taxa in a community and the sum of all t equals T. Thus, the relative contribution that the ith taxon makes towards T, defined here as τ_i, was calculated as:

$$\tau_i = \frac{p_i t_i}{\sum_{i=1}^{n} p_i t_i} \qquad 3)$$

As each τ_i is a fraction of T, we reformulate the abundance distribution for the community, C, as an abundance distribution with respect to τ (trait contribution distribution), such that:

$$C_{\tau,all} = \left\{\tau \middle| \tau_i \geq 0 \; \forall \; \tau_i; \textstyle\sum_{i=1}^{n} \tau_j = 1\right\} \qquad (4.1$$

and

$$C_\tau = \left\{\tau \in C_{\tau,all} \middle| \tau_i > 0 \; \forall \; \tau_i; \textstyle\sum_{i=1}^{\nu} \tau_i = 1\right\} \qquad (4.2$$

where again, τ_i is the relative contribution by the ith taxon to T, such that all τ sum to equal 1. The community represented in equation 4.1 considers the situation where τ can equal 0 because the ith

taxon has a p_i>0 but may not contribute to T (t_i=0). The community represented in equation 4.2 is a subset of equation 4.1, where C_τ contains only taxa from $C_{\tau,all}$ with t>0. As such, we adopted the variable, v, which represents the richness of taxa in C_τ. Note that equation 4.1 and 4.2 equal when all taxa contribute to T (t>0).

The necessity for differentiating equation 4.1 and equation 4.2 is that the trait contribution distribution in equation 4.2 is consistent with attributes of a community. Specifically, equation 4.2 does not include absent taxa which are not incorporated in conventional diversity metrics (20, 21). Thus, we utilized a parametric approach for characterizing parameters of diversity and evenness with respect to equation 4.2 (13). Diversity in trait-contributing taxa was determined as:

$$H_\tau = \begin{cases} \frac{1-\sum_{i=1}^{v} \tau_i{}^{\alpha}}{\alpha-1} & \alpha \neq 1 \\ \sum_{i=1}^{v} -\tau_i \log \tau_i & \alpha = 1 \end{cases} \quad (5$$

where α is a weighting parameter that defines the importance of taxa contributing less to T compared to taxa which contribute more. When α=0, H_τ simplifies to v-1, or the richness of trait-containing taxa minus one. When α=1, H_τ simplifies to Shannon's index. When α=2, H_τ simplifies to Simpson's index. The first scenario represents the least sensitive weighting towards relative trait contribution as it effectively measures how many taxa contain a trait. In contrast, increasing α decreases the sensitivity of H_τ to taxa which contribute less to T. As, our definition of functional redundancy is how evenly different taxa contribute to the community-level total trait within the community, we calculated a theoretical maximum for H_τ which assumes that trait level, t_i, is evenly distributed in equation 4 such that:

$$C_{\tau,E} = \left\{\tau \middle| \tau_i = \frac{1}{n} \ \forall \ \tau_i; \sum_{i=1}^{v} \tau_i = 1\right\} \quad (6$$

Implicitly, equation 6 assumes v=n, as this is the only scenario where the condition $\sum_{i=1}^{v} \tau_i = 1$ is held true. Thus, H_E is derived by calculating equation 5 using equation 6. As evenness is the ratio between observed diversity and the theoretical maximum diversity, we calculated functional redundancy, R, as:

$$R = \frac{H_\tau}{H_E} \quad (7$$

Functional Redundancy's Dependency on Diversity Continuum

We wanted to observe the effect that different diversity metrics (i.e., different values of α in equation 5) had on R. This was performed by calculating R with a fixed community and varying α from 0 to 2. We further characterized sensitivity in R with changes in community richness while fixing the trait-containing taxa (i.e., equation 4 constant while equation 1 changes). This scenario evaluated the sensitivity in H_E to equation 5 for different α while maintaining a constant H_τ. C_τ was defined as a lognormally-distributed community (32) following the functional form:

$$S(r) = S_0 e^{-a^2 r^2} \quad (8$$

where S_0 was the maximum abundance, r was the ith octave, and a was the inverse width of the lognormal distribution. Values for equation 8 were a=0.2, r spanned between 0 to 9 (v=10), and S_0=1. $S(r)$ was then normalized by the sum of abundances across all r so that the condition, $\sum_{i=1}^{v} \tau_i = 1$, was met. Afterwards, we dynamically increased values of n from 10 to 100 (lognormal-evenly distributed increments) for generating the theoretical, maximally diverse trait contribution distributions (equation 6). R was then calculated while keeping the H_τ at a fixed value. This exercise was performed for α spanning from values 0 to 2 at increments of 0.01.

Functional Redundancy Against Trait Vulnerability Simulations

We generated artificial communities such that the variables of community richness, diversity (with respect to *p*), and *t* were varied over a dynamic range. Community richness, *n*, was randomly assigned a value from 30 to 100 for individual communities. The relative abundance, *p*, for individual taxa within a community were then defined using equation 8. Values of *a* where randomly selected from 0 (even) to 0.4 (operationally more uneven) at 0.01 intervals. After establishing taxa relative abundances, we prescribed levels of trait to individual taxa. Level of trait, *t*, was assigned a value between 0 (does not contain) and 1 (maximum level) at intervals of 0.01. We randomly selected one of three scenarios in the assignment of *t*. The first scenario considered every taxon containing the trait, where every taxon had the trait greater than 0. The second scenario had 50% of the taxa containing the trait at a random level greater than 0 while the other 50% did not contain the trait. The last scenario had 20% of taxa containing the trait at a random level greater than 0 while 80% of taxa did not have the trait. In total, 10,000 artificial communities were generated with this approach. For each artificial community, functional redundancy with equations 1-8. For comparison, we calculated *R* based on Ricotta et al. (2016) (using code published in Appendix S1) (11). In our calculations of Rao's functional diversity, we utilized Euclidean distances.

We performed two separate simulations with the artificially generated communities described above. The first simulation varied α from 0 to 2 in equation 5 to determine which α maximized the dynamic range in observed functional redundancy. In this analysis, we excluded scenarios where R=0 and R=1. As functional redundancy spanned ~10 orders of magnitude, we reported the range after taking the $\log_{10}$ functional redundancy. The second simulation caused random taxon extinction events within the artificial communities described above. C_τ was

determined for individual artificial communities with equations 1-4. Taxon extinction events were simulated by randomly removing the same taxa from C (equation 1) and C_τ (equation 4). If a taxon in C did not contain the trait, then no taxa were removed from C_τ. After each taxon extinction event, the total τ in C_τ was determined by summing the remaining elements within C_τ. Random taxon extinction events continued until the sum of τ remaining in C_τ was >95% from starting value of τ (i.e, τ=1). Trait robustness to extinctions was then defined as the fraction of taxon richness (n) which went extinct prior to 95% of the trait being lost. The extinction simulation was performed 100 times for each of the individual 10,000 artificial communities. The trait robustness generated from the 100 simulations were then averaged for each of the individual 10,000 artificial communities.

A Case Study of Functional Redundancy in the Global Ocean Nitrogen Cycle

Draft metagenome-assembled genomes (MAGs) from (23) were downloaded from NCBI (38). In addition, MAG completeness, MAG relative abundance estimates, ocean depths, and ocean regions, defined in (23), were directly downloaded from Figshare (https://doi.org/10.6084/m9.figshare.5188273). We tabulated nitrogen-cycle marker genes in individual MAGs by blasting MAG proteins against nitrogen-cycle marker gene databases using the BLASTP algorithm (E-value=10^{-10}) (39). Nitrogen cycle marker genes were categorized into eight categories: N_2 fixation (*nifH*), nitrification (*amoA*, *hao*), NO_3 reduction (*napA*, *narG*), dissimilatory NO_3 reduction (*nrfA*), assimilatory NO_3/NO_2 reduction (*narB*, *nasA*, *nasB*, and *nirB*), NH_4^+ assimilation (*gdhA*, *glnA*), N remineralization (*gltB*), and denitrification (*nirK*, *nirS*, *norB*, and *nosZ*) (22). Individual BLAST databases were constructed for each nitrogen cycle category. Gene names associated with individual categories were searched for in the Swiss-Prot database (40). All proteins matching gene names were subsequently downloaded and used in

BLAST database construction. The number of matching genes for individual MAGs were normalized by the MAG completeness (fraction) to account for incomplete binning and assembly. Functional redundancy was then calculated for individual stations, at individual depths, for each nitrogen cycle category using equations 1-7. Lastly, Table S1 contains protein names, gene names, corresponding EC, and entry name for all genes used in the above analysis.

Data Availability

We provided a function for calculating functional redundancy with TCE and an example script at https://github.com/taylorroyalty/functional_redundancy_script.

Acknowledgments

Funding for this project was provided by a C-DEBI graduate fellowship to TMR. This is C-DEBI contribution number [to be assigned upon manuscript acceptance]. This work was supported by the U.S. Department of Energy, Office of Science, Office of Biological and Environmental Research, Genomic Science Program under Award Number DE-SC0020369. Lastly, we thank Dr. Karen Lloyd for providing feedback on this manuscript.

References

1. Martiny AC, Treseder K, Pusch G. 2013. Phylogenetic conservatism of functional traits in microorganisms. ISME J 7:830–838.

2. Royalty TM, Steen AD. 2019. Quantitatively Partitioning Microbial Genomic Traits among Taxonomic Ranks across the Microbial Tree of Life. mSphere 4:e00446-19.

3. Coles VJ, Stukel MR, Brooks MT, Burd A, Crump BC, Moran MA, Paul JH, Satinsky BM, Yager PL, Zielinski BL, Hood RR. 2017. Ocean biogeochemistry modeled with emergent trait-based genomics. Science (80-) 358:1149–1154.

4. Sunagawa S, Coelho LP, Chaffron S, Kultima JR, Labadie K, Salazar G, Djahanschiri B, Zeller G, Mende DR, Alberti A, Cornejo-Castillo FM, Costea PI, Cruaud C, d'Ovidio F, Engelen S, Ferrera I, Gasol JM, Guidi L, Hildebrand F, Kokoszka F, Lepoivre C, Lima-Mendez G, Poulain J, Poulos BT, Royo-Llonch M, Sarmento H, Vieira-Silva S, Dimier C, Picheral M, Searson S, Kandels-Lewis S, Bowler C, de Vargas C, Gorsky G, Grimsley N, Hingamp P, Iudicone D, Jaillon O, Not F, Ogata H, Pesant S, Speich S, Stemmann L, Sullivan MB, Weissenbach J, Wincker P, Karsenti E, Raes J, Acinas SG, Bork P, Boss E, Bowler C, Follows M, Karp-Boss L, Krzic U, Reynaud EG, Sardet C, Sieracki M, Velayoudon D. 2015. Structure and function of the global ocean microbiome. Science (80-) 348:1261359–1261359.

5. Louca S, Martiny AC, Polz MF, Doolittle WF, Nelson MB, Hahn AS, Rubin I, Mazel F, Hawley AK, Connor MIO, Crowe SA, Hallam SJ. 2018. Function and functional redundancy in microbial communities. Nat Ecol Evol 2:936–943.

6. Naeem S. 1998. Species redundancy and ecosystem reliability. Conserv Biol 12:39–45.

7. Hunting ER, Vijver MG, van der Geest HG, Mulder C, Kraak MHS, Breure AM, Admiraal W. 2015. Resource niche overlap promotes stability of bacterial community metabolism in experimental microcosms. Front Microbiol 6:1–7.

8. Teeling H, Fuchs BM, Becher D, Klockow C, Gardebrecht A, Bennke CM, Kassabgy M, Huang S, Mann AJ, Waldmann J, Weber M, Klindworth A, Otto A, Lange J, Bernhardt J, Reinsch C, Hecker M, Peplies J, Bockelmann FD, Callies U, Gerdts G, Wichels A, Wiltshire KH, Glöckner FO, Schweder T, Amann R. 2012. Substrate-Controlled Succession of Marine Bacterioplankton Populations Induced by a Phytoplankton Bloom. Science (80-) 336:608–611.

9. Heintz-Buschart A, Wilmes P. 2018. Human Gut Microbiome: Function Matters. Trends Microbiol 26:563–574.

10. Rao R. 1982. Diversity and Dissimilarity Coefficients: A Unified Approach. Theor Popul Biol 21:24–43.

11. Ricotta C, de Bello F, Moretti M, Caccianiga M, Cerabolini BEL, Pavoine S. 2016. Measuring the functional redundancy of biological communities: a quantitative guide. Methods Ecol Evol 7:1386–1395.

12. Mouillot D, Villéger S, Parravicini V, Kulbicki M, Arias-González JE, Bender M, Chabanet P, Floeter SR, Friedlander A, Vigliola L, Bellwood DR. 2014. Functional over-redundancy and high functional vulnerability in global fish faunas on tropical reefs. Proc Natl Acad Sci U S A 111:13757–13762.

13. Ricotta C, Szeidl L. 2006. Towards a unifying approach to diversity measures: Bridging the gap between the Shannon entropy and Rao's quadratic index. Theor Popul Biol

70:237–243.

14. Villéger S, Mason NWH, Mouillot D. 2008. New Mulitdimensional Functional Diversity Indicies for a Muiltifaceted Framework in Functional Ecology. Ecology 39:2290–2301.

15. Staley J, Konopka A. 1985. Measurement of In Situ Activities of Nonphotosynthetic Microorganisms in Aquatic and Terrestrial Habitats. Annu Rev Microbiol 39:321–346.

16. Allison SD, Martiny JBH. 2009. Resistance, resilience, and redundancy in microbial communities. Light Evol 2:149–166.

17. Delgado-Baquerizo M, Giaramida L, Reich PB, Khachane AN, Hamonts K, Edwards C, Lawton LA, Singh BK. 2016. Lack of functional redundancy in the relationship between microbial diversity and ecosystem functioning. J Ecol 104:936–946.

18. Krause S, Le Roux X, Niklaus PA, van Bodegom PM, Lennon T. JT, Bertilsson S, Grossart HP, Philippot L, Bodelier PLE. 2014. Trait-based approaches for understanding microbial biodiversity and ecosystem functioning. Front Microbiol 5:1–10.

19. Martiny JBH, Jones SE, Lennon JT, Martiny AC. 2015. Microbiomes in light of traits: A phylogenetic perspective. Science (80-) 350:aac9323.

20. Patil GP, Taillie C. 1982. Diversity as a concept and its measurement. J Am Stat Assoc 77:548–561.

21. McGill BJ, Etienne RS, Gray JS, Alonso D, Anderson MJ, Benecha HK, Dornelas M, Enquist BJ, Green JL, He F, Hurlbert AH, Magurran AE, Marquet PA, Maurer BA, Ostling A, Soykan CU, Ugland KI, White EP. 2007. Species abundance distributions: Moving beyond single prediction theories to integration within an ecological framework.

Ecol Lett 10:995–1015.

22. Pajares S, Ramos R. 2019. Processes and Microorganisms Involved in the Marine Nitrogen Cycle: Knowledge and Gaps. Front Mar Sci 6.

23. Tully BJ, Graham ED, Heidelberg JF. 2018. The reconstruction of 2,631 draft metagenome-assembled genomes from the global oceans. Sci Data 5:1–8.

24. Falkowski PG, Fenchel T, Delong EF. 2008. The Microbial Engines That Drive Earth's Biogeochemical Cycles. Science (80-) 320:1034–1039.

25. Malik AA, Martiny JBH, Brodie EL, Martiny AC, Treseder KK, Allison SD. 2019. Defining trait-based microbial strategies with consequences for soil carbon cycling under climate change. ISME J 445866.

26. Baker BJ, Lazar CS, Teske AP, Dick GJ. 2015. Genomic resolution of linkages in carbon, nitrogen, and sulfur cycling among widespread estuary sediment bacteria. Microbiome 3:14.

27. Anantharaman K, Brown CT, Hug LA, Sharon I, Castelle CJ, Probst AJ, Thomas BC, Singh A, Wilkins MJ, Karaoz U, Brodie EL, Williams KH, Hubbard SS, Banfield JF. 2016. Thousands of microbial genomes shed light on interconnected biogeochemical processes in an aquifer system. Nat Commun 7:13219.

28. Pielou EC. 1966. The measurement of diversity in different types of biological collections. J Theor Biol 13:131–144.

29. Hubert C. 2009. A Constant Flux of Diverse. Program 1541:1541–1544.

30. McPherson JM, Yeager LA, Baum JK. 2018. A simulation tool to scrutinise the behaviour

of functional diversity metrics. Methods Ecol Evol 9:200–206.

31. Tilman D. 2001. Functional Diversity. Encycl Biodivers Second Ed 3:587–596.

32. Magurran AE. 1988. Ecological Diversity and Its Measurement, 1st ed. Croom Helm Ltd.

33. Wuchter C, Abbas B, Coolen MJL, Herfort L, Van Bleijswijk J, Timmers P, Strous M, Teira E, Herndl GJ, Middelburg JJ, Schouten S, Damsté JSS. 2006. Archaeal nitrification in the ocean. Proc Natl Acad Sci U S A 103:12317–12322.

34. Thompson LR, Sanders JG, McDonald D, Amir A, Ladau J, Locey KJ, Prill RJ, Tripathi A, Gibbons SM, Ackermann G, Navas-Molina JA, Janssen S, Kopylova E, Vázquez-Baeza Y, González A, Morton JT, Mirarab S, Xu ZZ, Jiang L, Haroon MF, Kanbar J, Zhu Q, Song SJ, Kosciolek T, Bokulich NA, Lefler J, Brislawn CJ, Humphrey G, Owens SM, Hampton-Marcell J, Berg-Lyons D, McKenzie V, Fierer N, Fuhrman JA, Clauset A, Stevens RL, Shade A, Pollard KS, Goodwin KD, Jansson JK, Gilbert JA, Knight R, Agosto Rivera JL, Al-Moosawi L, Alverdy J, Amato KR, Andras J, Angenent LT, Antonopoulos DA, Apprill A, Armitage D, Ballantine K, Bárta J, Baum JK, Berry A, Bhatnagar A, Bhatnagar M, Biddle JF, Bittner L, Boldgiv B, Bottos E, Boyer DM, Braun J, Brazelton W, Brearley FQ, Campbell AH, Caporaso JG, Cardona C, Carroll JL, Cary SC, Casper BB, Charles TC, Chu H, Claar DC, Clark RG, Clayton JB, Clemente JC, Cochran A, Coleman ML, Collins G, Colwell RR, Contreras M, Crary BB, Creer S, Cristol DA, Crump BC, Cui D, Daly SE, Davalos L, Dawson RD, Defazio J, Delsuc F, Dionisi HM, Dominguez-Bello MG, Dowell R, Dubinsky EA, Dunn PO, Ercolini D, Espinoza RE, Ezenwa V, Fenner N, Findlay HS, Fleming ID, Fogliano V, Forsman A, Freeman C, Friedman ES, Galindo G, Garcia L, Garcia-Amado MA, Garshelis D, Gasser

RB, Gerdts G, Gibson MK, Gifford I, Gill RT, Giray T, Gittel A, Golyshin P, Gong D, Grossart HP, Guyton K, Haig SJ, Hale V, Hall RS, Hallam SJ, Handley KM, Hasan NA, Haydon SR, Hickman JE, Hidalgo G, Hofmockel KS, Hooker J, Hulth S, Hultman J, Hyde E, Ibáñez-Álamo JD, Jastrow JD, Jex AR, Johnson LS, Johnston ER, Joseph S, Jurburg SD, Jurelevicius D, Karlsson A, Karlsson R, Kauppinen S, Kellogg CTE, Kennedy SJ, Kerkhof LJ, King GM, Kling GW, Koehler A V., Krezalek M, Kueneman J, Lamendella R, Landon EM, Lanede Graaf K, LaRoche J, Larsen P, Laverock B, Lax S, Lentino M, Levin II, Liancourt P, Liang W, Linz AM, Lipson DA, Liu Y, Lladser ME, Lozada M, Spirito CM, MacCormack WP, MacRae-Crerar A, Magris M, Martín-Platero AM, Martín-Vivaldi M, Martínez LM, Martínez-Bueno M, Marzinelli EM, Mason OU, Mayer GD, McDevitt-Irwin JM, McDonald JE, McGuire KL, McMahon KD, McMinds R, Medina M, Mendelson JR, Metcalf JL, Meyer F, Michelangeli F, Miller K, Mills DA, Minich J, Mocali S, Moitinho-Silva L, Moore A, Morgan-Kiss RM, Munroe P, Myrold D, Neufeld JD, Ni Y, Nicol GW, Nielsen S, Nissimov JI, Niu K, Nolan MJ, Noyce K, O'Brien SL, Okamoto N, Orlando L, Castellano YO, Osuolale O, Oswald W, Parnell J, Peralta-Sánchez JM, Petraitis P, Pfister C, Pilon-Smits E, Piombino P, Pointing SB, Pollock FJ, Potter C, Prithiviraj B, Quince C, Rani A, Ranjan R, Rao S, Rees AP, Richardson M, Riebesell U, Robinson C, Rockne KJ, Rodriguezl SM, Rohwer F, Roundstone W, Safran RJ, Sangwan N, Sanz V, Schrenk M, Schrenzel MD, Scott NM, Seger RL, Seguinorlando A, Seldin L, Seyler LM, Shakhsheer B, Sheets GM, Shen C, Shi Y, Shin H, Shogan BD, Shutler D, Siegel J, Simmons S, Sjöling S, Smith DP, Soler JJ, Sperling M, Steinberg PD, Stephens B, Stevens MA, Taghavi S, Tai V, Tait K, Tan CL, Taş N, Taylor DL, Thomas T, Timling I, Turner BL, Urich T, Ursell LK, Van Der Lelie D, Van Treuren W, Van

Zwieten L, Vargas-Robles D, Thurber RV, Vitaglione P, Walker DA, Walters WA, Wang S, Wang T, Weaver T, Webster NS, Wehrle B, Weisenhorn P, Weiss S, Werner JJ, West K, Whitehead A, Whitehead SR, Whittingham LA, Willerslev E, Williams AE, Wood SA, Woodhams DC, Yang Y, Zaneveld J, Zarraonaindia I, Zhang Q, Zhao H. 2017. A communal catalogue reveals Earth's multiscale microbial diversity. Nature 551:457–463.

35. Steen AD, Crits-Christoph A, Carini P, DeAngelis KM, Fierer N, Lloyd KG, Cameron Thrash J. 2019. High proportions of bacteria and archaea across most biomes remain uncultured. ISME J 13:3126–3130.

36. Lloyd KG, Steen AD, Ladau J, Yin J, Crosby L. 2018. Phylogenetically Novel Uncultured Microbial Cells Dominate Earth Microbiomes. mSystems 3:1–12.

37. Musat N, Foster R, Vagner T, Adam B, Kuypers MMM. 2012. Detecting metabolic activities in single cells, with emphasis on nanoSIMS. FEMS Microbiol Rev 36:486–511.

38. Federhen S. 2012. The NCBI Taxonomy database. Nucleic Acids Res 40:136–143.

39. Clark K, Karsch-Mizrachi I, Lipman DJ, Ostell J, Sayers EW. 2019. GenBank. Nucleic Acids Res 47:D94–D99.

40. Bairoch A, Apweiler R. 2000. The SWISS-PROT protein sequence database and its supplement TrEMBL in 2000. Nucleic Acids Res 28:45–48.

Tables

Table 1. A summary of marker gene sequences used in the BLASTP analysis of *TARA Oceans* MAGs. All marker genes were downloaded from Swiss-Prot.

Pathway	Gene Names	EC Number	# Marker Genes
N Remineralization	*gltB*	1.4.1.13	14
N Fixation	*nifH*	1.18.6.1	127
Nitrification	*amoA*	1.14.99.39	2
	hoa	1.7.2.6	1
NO_3^- Reduction	*napA*	1.9.6.1	136
	narG	1.7.5.1	13
Dissimilatory NO_3^- Reduction	*nrfA*	1.7.2.2	77
Assimilatory NO_3^-/NO_2^- Reduction	*narB*	1.7.5.1	3
	nasA	1.7.7.2	1
	nasB	1.7.1.4	3
	nirB	1.7.1.15	5
NH_4^+ Assimilation	*gdhA*	1.4.1.3	14
	glnA	6.3.1.2	173
Denitrification	*nirK*	1.7.2.1	7
	nirS	1.7.2.1; 1.7.99.1	4
	norB	1.7.2.5	2
	nosZ	1.7.2.4	11

Figures

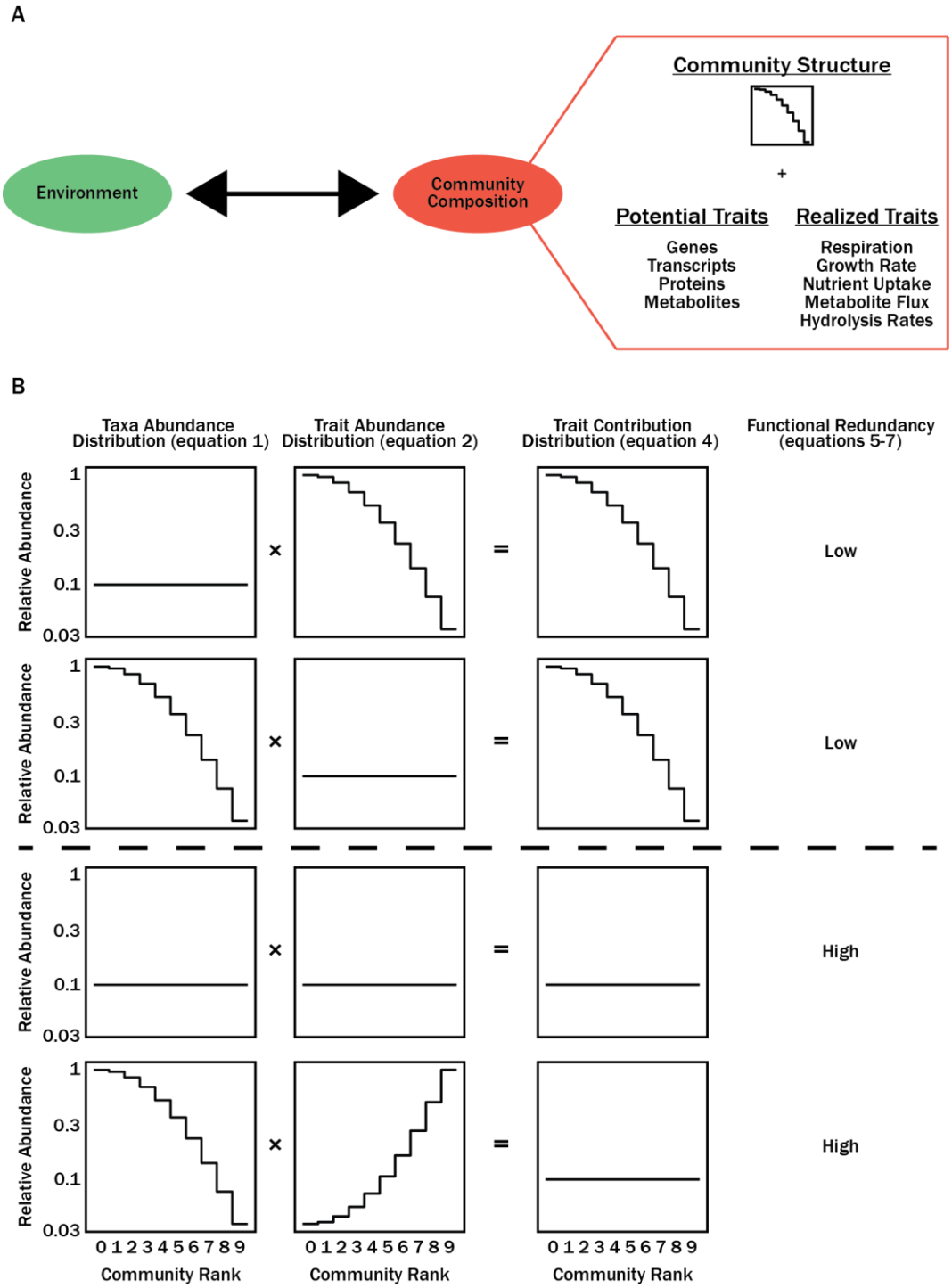

Fig 1.

The interplay between environmental parameters and microbial community composition requires an understanding of both community taxa abundances as well as trait levels for respective taxa (A). Community taxa abundance and relative trait level are scalable and provide a measure for the contribution that different taxa have to the total community level trait (B).

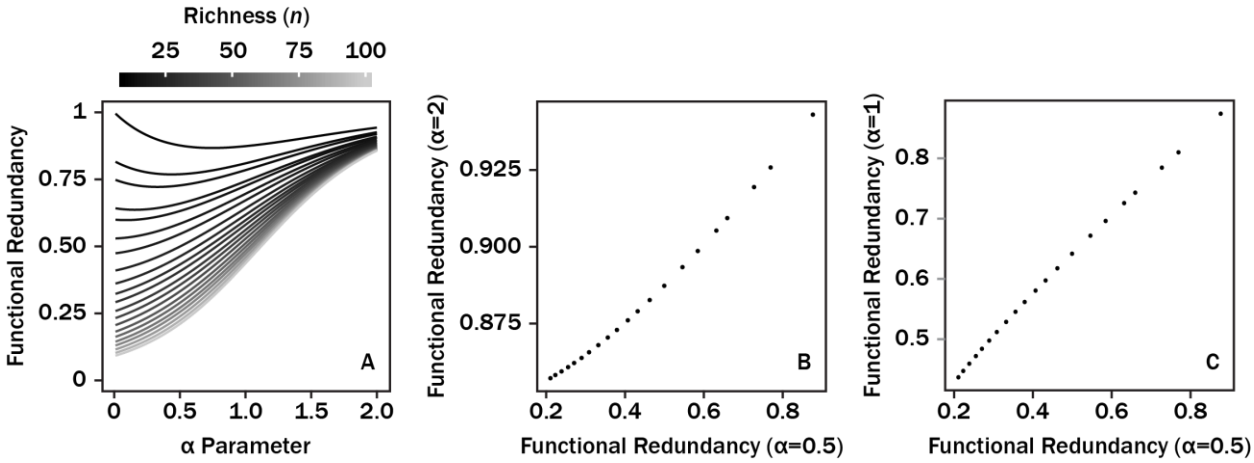

Fig 2.

The sensitivity in functional redundancy in response changing α in equation 5 (**A**). Contours correspond to increasing community richness (n) while maintaining the structure of the trait-containing community. Comparisons between contours from (**A**) when α=0.5 and α=2 (**B**) as well as when α=0.5 and α=1 (**C**).

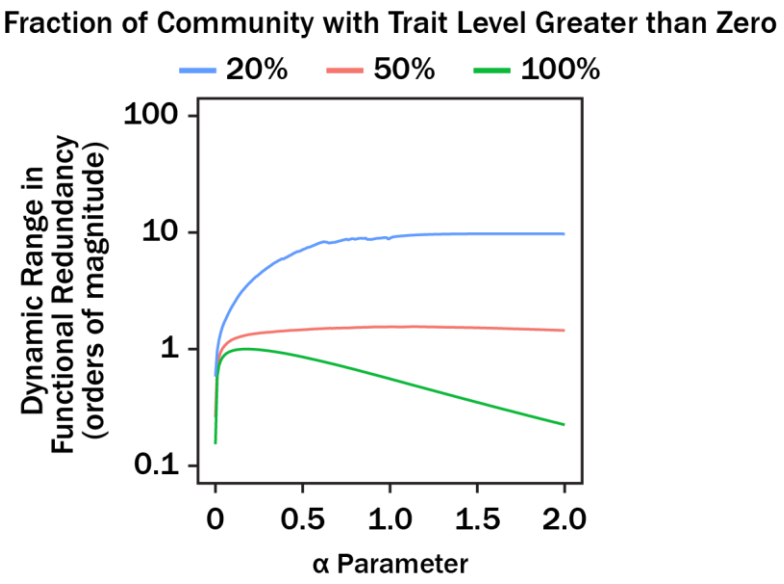

Fig 3.

The dynamic range in functional redundancy for randomly generated artificial communities as a function of α selected for equation 5. Contours correspond to the fraction of the community containing a trait. Note that at $\alpha = 1$ and the fraction of community was 20%, the dynamic range was smoothed due to precision error from the log-transformation in equation 5 when calculating function redundancy. All other data reflect results from artificial communities.

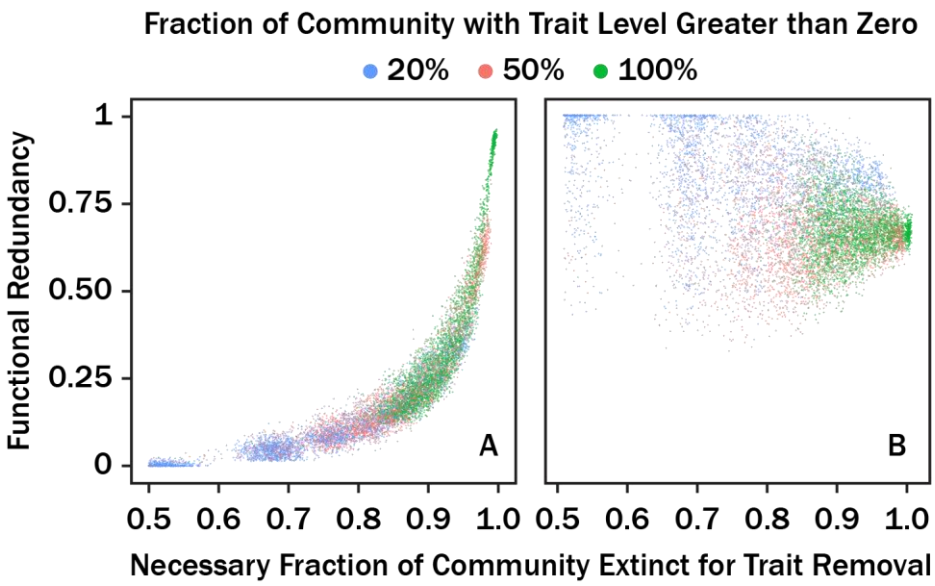

Fig 4.

A comparison of functional redundancy versus the fraction of community richness that goes randomly extinct prior to a 95% of trait level being lost on the community level. Functional redundancy was calculated with equations 1-7 (α=0.5) (**A**) as well as using the method in (11) (**B**).

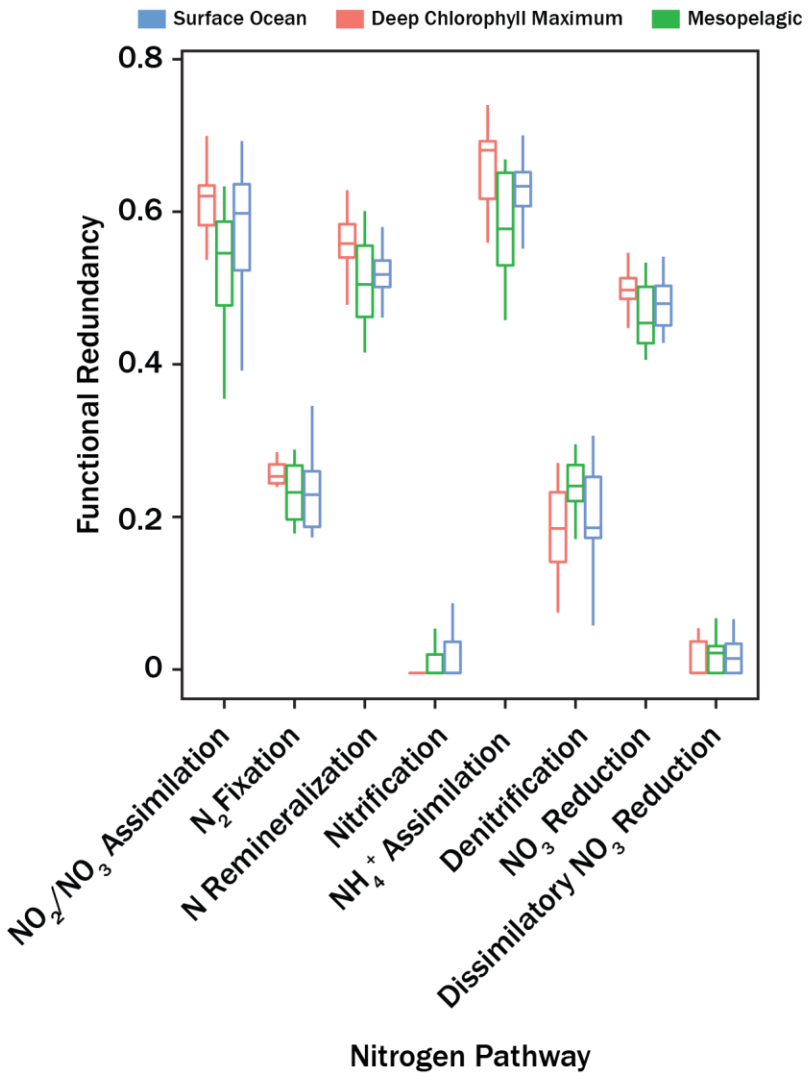

Fig 5.

Boxplots showing functional redundancy calculated for eight nitrogen-transforming pathways in *TARA Oceans* draft MAGs. Different colors correspond to sample depth. Whiskers correspond to 150% of the inter-quantile region.

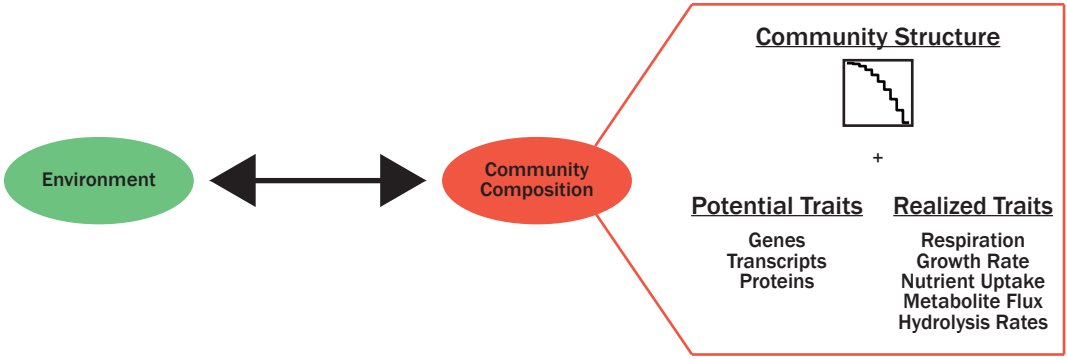
A
Environment
Community Composition
Community Structure
+
Potential Traits
Genes
Transcripts
Proteins
Realized Traits
Respiration
Growth Rate
Nutrient Uptake
Metabolite Flux
Hydrolysis Rates

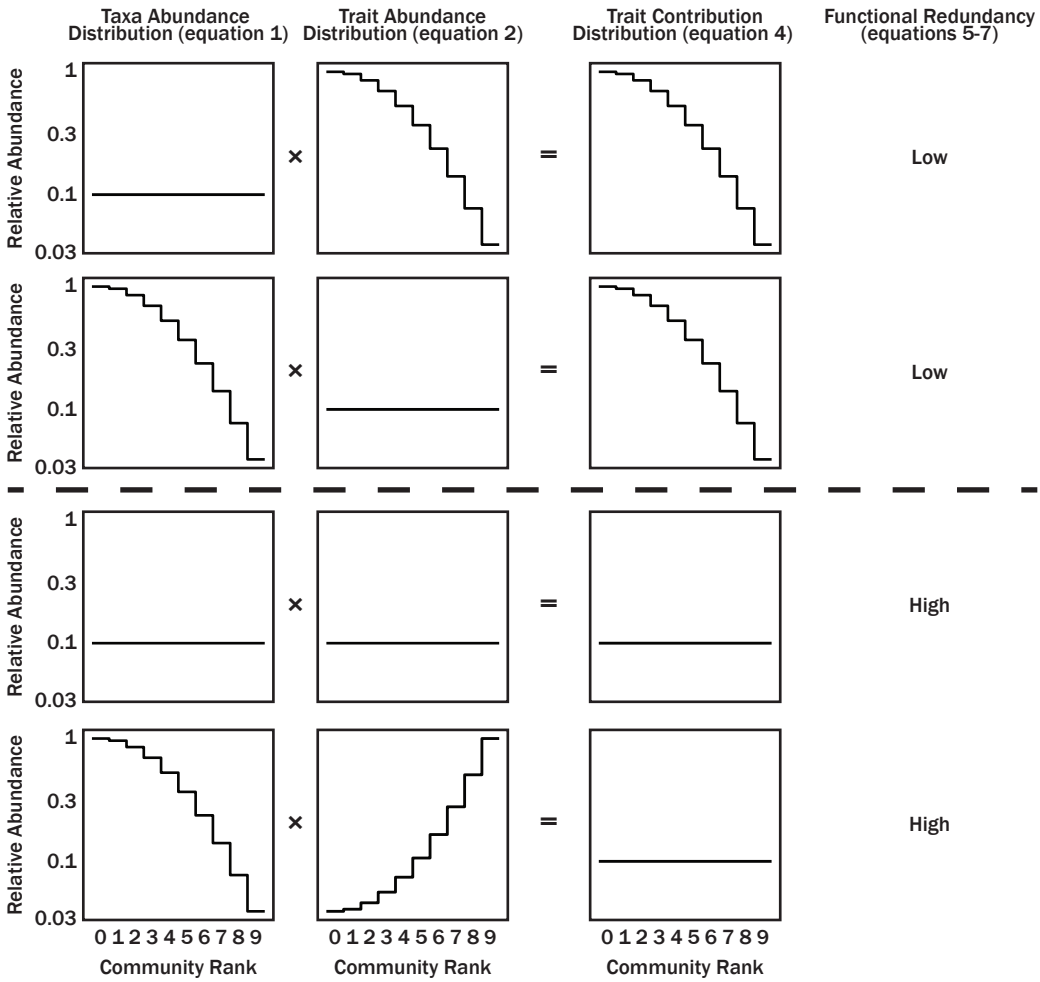
B
Taxa Abundance Distribution (equation 1)
Trait Abundance Distribution (equation 2)
Trait Contribution Distribution (equation 4)
Functional Redundancy (equations 5-7)
Relative Abundance
1
0.3
0.1
0.03
×
=
Low
Low
High
High
0 1 2 3 4 5 6 7 8 9
Community Rank

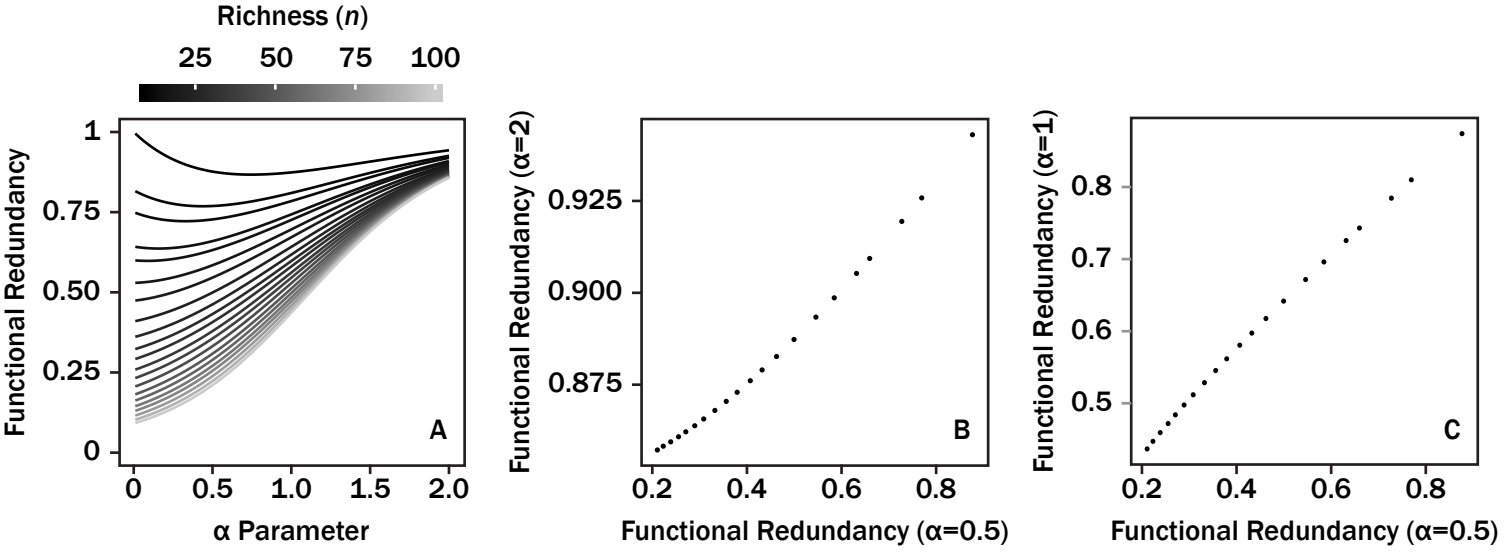
Richness (n)
25
50
75
100
Functional Redundancy
1
0.75
0.50
0.25
0
0
0.5
1.0
1.5
2.0
α Parameter
A
Functional Redundancy (α=2)
0.925
0.900
0.875
0.2
0.4
0.6
0.8
Functional Redundancy (α=0.5)
B
Functional Redundancy (α=1)
0.8
0.7
0.6
0.5
0.2
0.4
0.6
0.8
Functional Redundancy (α=0.5)
C

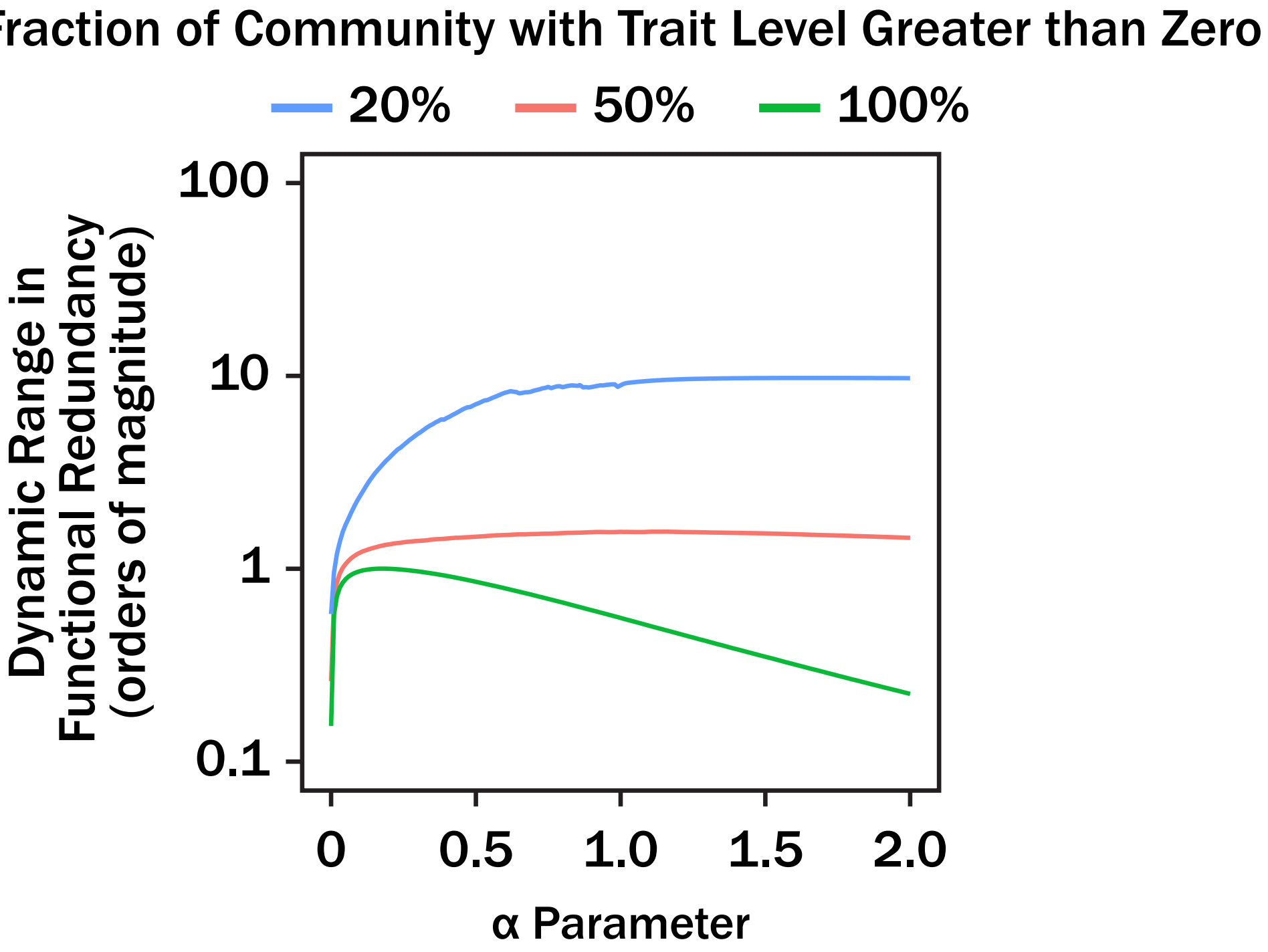
Fraction of Community with Trait Level Greater than Zero
20%
50%
100%
Dynamic Range in Functional Redundancy (orders of magnitude)
100
10
1
0.1
0
0.5
1.0
1.5
2.0
α Parameter

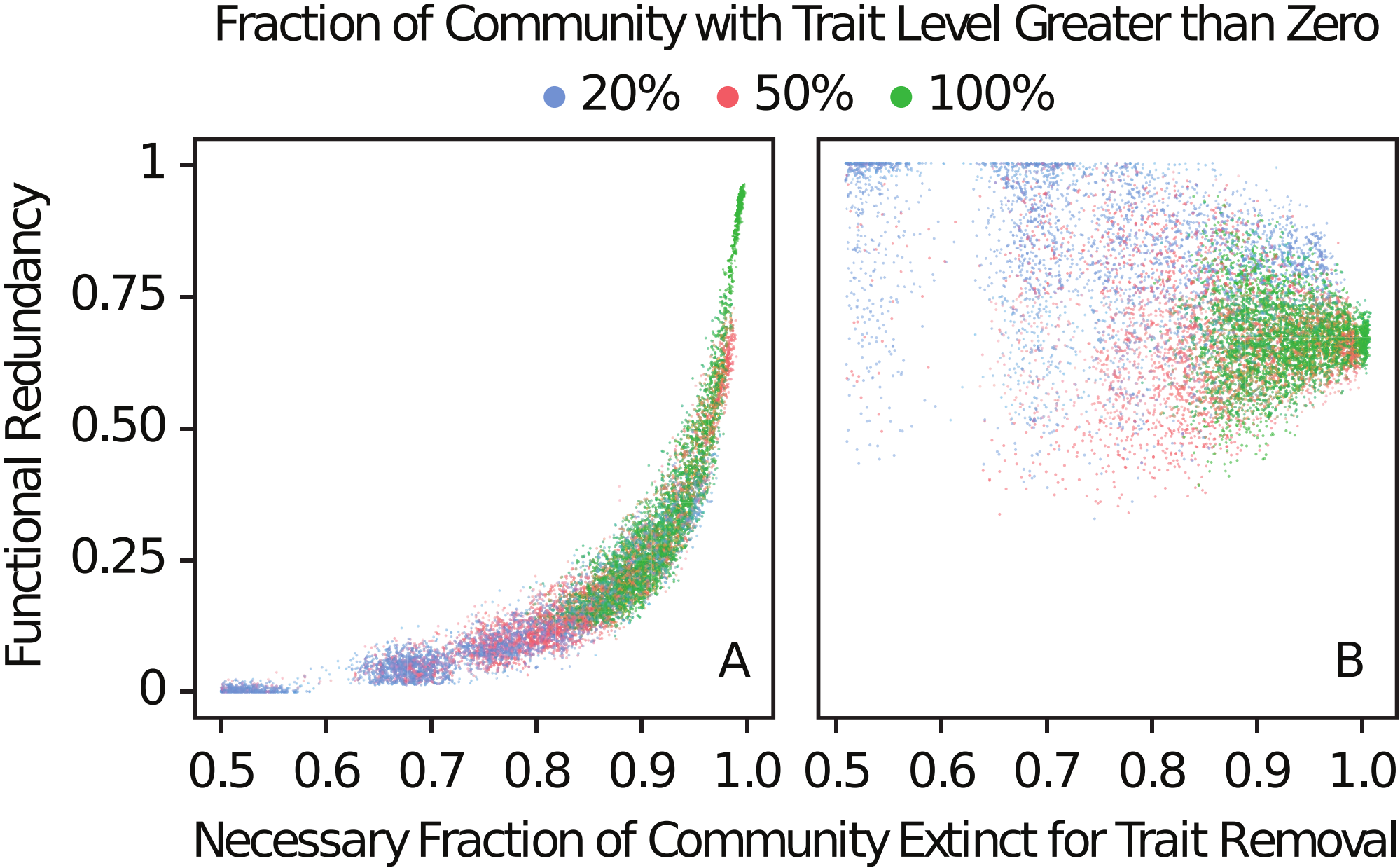
Fraction of Community with Trait Level Greater than Zero
20%
50%
100%
Functional Redundancy
1
0.75
0.50
0.25
0
A
B
0.5
0.6
0.7
0.8
0.9
1.0
Necessary Fraction of Community Extinct for Trait Removal

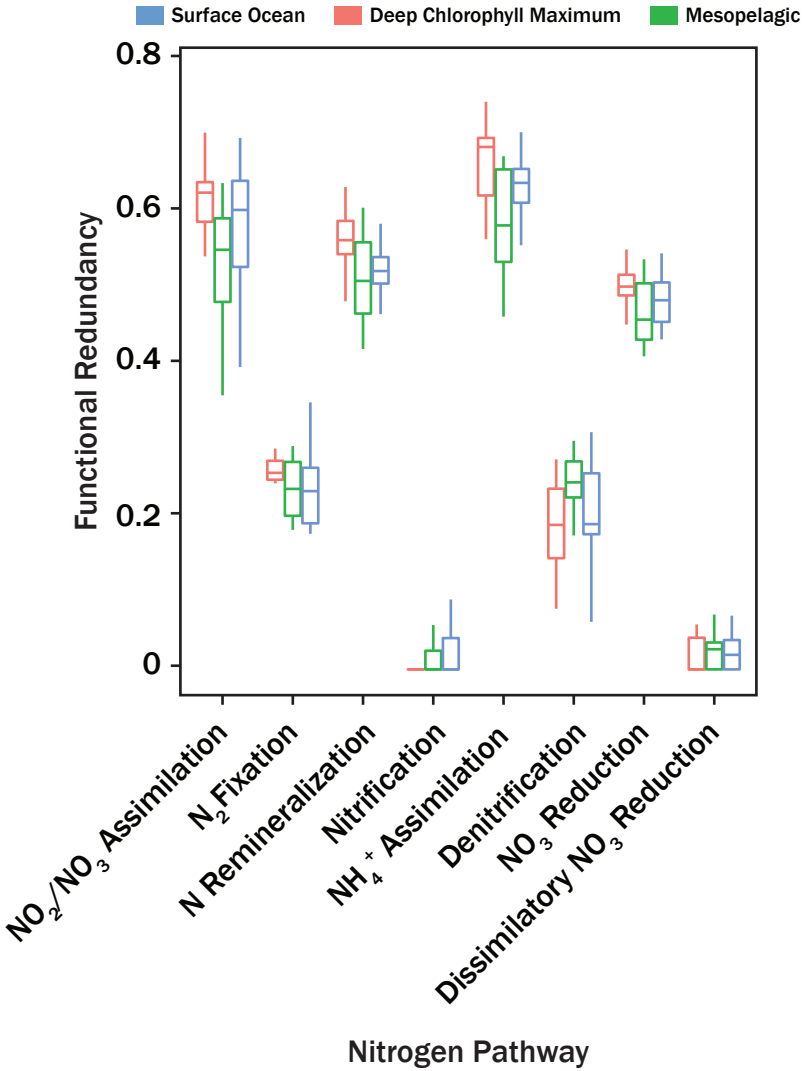
Surface Ocean
Deep Chlorophyll Maximum
Mesopelagic
Functional Redundancy
0.8
0.6
0.4
0.2
0
NO_2/NO_3 Assimilation
N_2 Fixation
N Remineralization
Nitrification
NH_4^+ Assimilation
Denitrification
NO_3 Reduction
Dissimilatory NO_3 Reduction
Nitrogen Pathway